Article

Not peer-reviewed version

Evaluation of Contrast-Enhanced Mammography and Development of Flowchart for BI-RADS Classification of Breast Lesions

Kristina Klarić *, Andrej Šribar, Anuška Budisavljević, Loredana Labinac Peteh, Petra Valković Zujić

Posted Date: 5 May 2023

doi: 10.20944/preprints202305.0284.v1

Keywords: breast cancer; contrast-enhanced mammography; magnetic resonance imaging

Article

Evaluation of Contrast-Enhanced Mammography and Development of Flowchart for BI-RADS Classification of Breast Lesions

Kristina Klarić [1,*], Andrej Šribar [2], Anuška Budisavljević [3], Loredana Labinac [4] and Petra Valković Zujić [5,6]

[1] Department of Radiology, Pula General Hospital, 52100 Pula, Croatia
[2] Clinic for Anaesthesiology, Resuscitation and Intensive care medicine, Dubrava Clinical Hospital, 10000 Zagreb, Croatia; andrej.sribar@gmail.com
[3] Department of Oncology, Pula General Hospital, 52100 Pula, Croatia; gigaab32@gmail.com
[4] Department of Pathology and Cytology, Pula General Hospital, 52100 Pula, Croatia; loredanalabinacpeteh@gmail.com
[5] Department of Radiology, Clinical Hospital Center Rijeka, 51000 Rijeka, Croatia; petra.valkovic.zujic@medri.uniri.hr
[6] Faculty of Medicine University of Rijeka, Brace Branchetta 20, 51000 Rijeka
* Correspondence: klarickristina8@gmail.com

Abstract: This study aimed to evaluate contrast-enhanced mammography (CEM) and compare breast lesions on CEM and breast magnetic resonance imaging (MRI) using 5 features. We propose to create a flowchart for BI-RADS classification of breast lesions on CEM based on the Kaiser score (KS) flowchart for breast MRI. Included were 68 subjects (women and men; median age 61.4 ± 11.6 years) who were suspected of having a malignant process in the breast based on digital mammography (MG) findings. The patients underwent breast ultrasound (US), CEM, MRI, and biopsy of the suspicious lesion. There were 47 patients with malignant lesions confirmed by biopsy and 21 patients with benign lesions, for each of which a KS was calculated. In the patients with malignant lesions, the MRI-derived KS was 9 (IQR 8-9), its CEM equivalent was 9 (IQR 8-9), and BI-RADS was 5 (IQR 4-5). In patients with benign lesions, MRI-derived KS was 3 (IQR 2-3), its CEM equivalent was 3 (IQR 1.7-5), and BI-RADS was 3 (IQR 0-4). There was no significant difference between the ROC-AUC of CEM and MRI (P=0.749). In conclusion, there were no significant differences in KS results between CEM and breast MRI. The KS flowchart is useful for evaluating breast lesions on CEM.

Keywords: breast cancer; contrast-enhanced mammography; magnetic resonance imaging

1. Introduction

Breast cancer is the most common cancer in the female population [1]. In 2020, 2 - 3 million new cases were diagnosed and 600, 000 deaths from breast cancer were recorded worldwide [1]. The incidence of breast cancer varies from 541/100 000 in high-income countries to 95/100 000 in low-income countries [2]. Due to population growth and ageing, there will be an estimated 3 million breast cancer cases and 1 million breast cancer-related deaths per year by 2040 [3]. Depending on the quality of screening programmes, approximately 70% of newly diagnosed cases are in the early stage, in which the disease is confined to the breast and regional lymph nodes while the remaining cases are metastatic breast cancer, in which the disease spreads widely [4,5]. Breast cancer is a highly heterogeneous disease with different subtypes, each having distinct clinicopathological features [4]. A metanalysis by Bernard et al examined the following risk factors for breast cancer: younger age at menarche, higher parity, older age at first birth, older age at menopause, body mass index, family history, alcohol use, oral contraceptive use, and menopausal hormone therapy [6]. Survival rates for

Preprints (www.preprints.org) | NOT PEER-REVIEWED | Posted: 5 May 2023 doi:10.20944/preprints202305.0284.v1

breast cancer depend on many factors including histologic and molecular subtype, stage of disease, quality of screening programmes, health care resources, and access to new breast cancer therapies [4]. In metastatic disease, the 5-year survival rate is 38% [5]. The 5-year survival rate for early breast cancer is approximately 95% in countries with high-quality cancer care [6].

The increasing incidence and mortality of breast cancer worldwide require continued research and investment to improve diagnostic techniques for the detection and characterization of breast lesions. CEM is a newer radiological diagnostic procedure used to detect and characterize breast lesions. It is based on imaging tumor blood vessels using an iodine contrast agent administered intravenously immediately before performing the mammogram. Research on the use of intravenous contrast in mammography began in 1985, with the performance of digital subtraction angiography of the breast, but this procedure was abandoned due to its invasiveness and suboptimal results [7]. The development of digital mammography, then the single-view temporal technique, and finally the dual-energy technique allowed the production of the first commercial system for performing CEM, which was approved by the US Food and Drug Administration in 2011 [8]. Breast MRI is another contrast-enhanced procedure that takes advantage of tumor angiogenesis to detect breast lesions and uses gadolinium-based contrast that accumulates in the cancer stroma. A systematic review and meta-analysis by Gelardi F. et al. showed that both CEM and MRI detect breast lesions with high sensitivity, with no significant difference in performance (97% and 96%, respectively) [9]. CEM has several advantages over MRI: it is better tolerated by patients, especially those with limited mobility or claustrophobia; there is no contraindication to CEM in patients with metal implants; the examination takes less time and reading the images is faster [10]. In addition to contrast imaging of the lesion in the breast, CEM also detects clusters of pathologic microcalcifications that can be biopsied by vacuum-assisted biopsy (VAB) [11].

To improve communication and understanding of findings between radiologists and clinicians, the American College of Radiology created the Breast Imaging Reporting and Data System (BI-RADS), which implies standardized terminology for grading lesions in the breast and is widely used in categorizing MG, breast US, and MRI findings. In 2022, the supplement to the 2013 ACR BI-RADS atlas for breast lesions was published on CEM [12]. However, the BI-RADS system does not include a clinical decision rule. Therefore, P.A.T. Baltzer et al. created a simple flowchart named after breast MRI pioneer Werner A. Kaiser, that guides the interpreting physician in two to three steps to a risk category that can then be translated into an objective diagnosis and management recommendation [13]. The KS flowchart is shown in Figure 1. In this study, we aimed to investigate whether a flowchart for BI-RADS classification of breast lesions for CEM could be based on the KS for MRI. First, we needed to evaluate the CEM and compare breast lesions on the CEM and MRI based on five features from the KS flowchart. If there is a high agreement between CEM and MRI, it is reasonable to assume that a similar flowchart can be created for CEM.

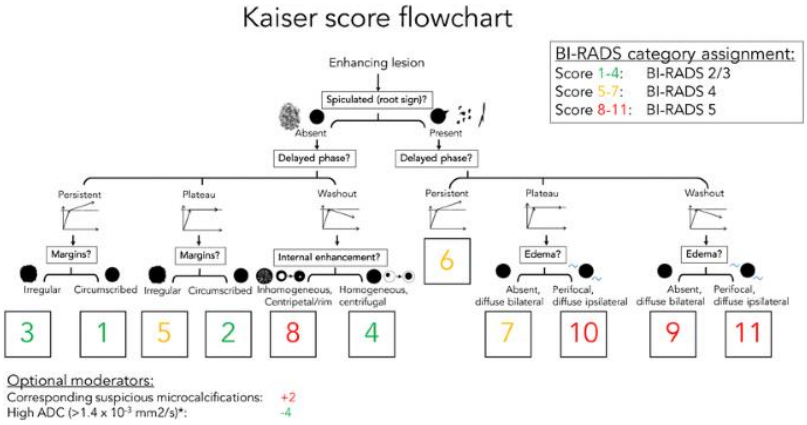

Figure 1. The Kaiser score flowchart. The diagnostic score ranging from 1 to 12, is associated with an increased risk of malignancy. If the score exceeds 4, a biopsy is recommended. https://dx.doi.org/10.26044/ecr2019/C-2750.

 doi:10.20944/preprints202305.0284.v1

2. Materials and methods

2.1. Study Design

This monocentric prospective study was approved by the Ethics Committee of Pula General Hospital (Registry Number 2168/01-59-79-19/1-21-8). All subjects who participated in the study read and signed the informed consent form. At our institution, MG is performed as part of screening (National Preventive Program for Early Detection of Breast Cancer) or as part of a diagnostic procedure in symptomatic patients. In the Republic of Croatia, the age of women included in the National Breast Cancer Early Detection Program ranges from 50 to 69 years, while patients with symptoms of breast disease can be younger.

2.2. Study Population

Sixty-eight subjects were included in the study (median age 61.4 ± 11.6 years). They had all undergone MG and were included in the study if mammographic findings were classified into one of three categories: BI-RADS 0, 4, or 5. All subjects with BI-RADS 0, 4, and 5 on MG underwent US, CEM, and MRI examinations at our institution. Exclusion criteria were contraindications to CEM and MRI (allergy, renal insufficiency, pregnancy/breastfeeding), findings without abnormal enhancement on CEM, subjects unable to undergo MRI (claustrophobia, metal implants), lack of pathohistological confirmation of the lesion in the breast, missing data for this study, subjects who denied participation in the study, subjects who continued treatment in another facility, and previous surgery or radiation, chemotherapy, or hormonal therapy for the treatment of breast cancer.

2.3. CEM and MRI Image Acquisition and Comparison

The MG was performed using the Selenia Dimensions digital mammography device (Hologic, Marlborough, Massachusetts, USA). MG was performed as part of the screening program using the full-field technique (FFDM), which consisted of two-dimensional craniocaudal and mediolateral oblique projections (CC and MLO) of the right and left breast. Diagnostic MG also included synthetic MG with layered (3D) breast imaging, in addition to 2D imaging. Breast US examinations were performed with the Acuson Sequoia ultrasound machine (Mountain View, California, USA), using a linear high-frequency probe (13-15 MHz). The CEM procedure was performed with the same digital mammography device and the protocol included: iodine-containing intravenous contrast agent Omnipaque 350 (Iohexol, GE Healthcare, Illinois, USA) or Xenetix 350 (Iobitridol, Guerbet, Lanester, France) with an application using an automated syringe to administer the of contrast agent bolus. The dose of the contrast agent was 1.5 ml/kg body weight at a rate of 3 ml/s. After a 2-minute break, necessary to saturate the breast parenchyma with contrast, the patients underwent four standard mammographic projections with the required breast compression: CC and MLO projection of the symptomatic breast and CC and MLO projection of the healthy breast, as well as delayed CC and MLO projections, of the symptomatic breast within 8 minutes of the start of the examination. Delayed radiographs were used to assess the dynamics of the contrast uptake of the lesion and compared with the same parameter of MRI. The time required to perform the CEM procedure was 8-10 minutes. MRI of the breast was performed on Aera 1.5 T Magnetome (Siemens Healthineers, Erlangen, Germany) with the patient in the prone position using a dedicated breast surface coil. A gadolinium contrast agent was injected (0.1 mmol/kg), and one pre-contrast and 6 post-contrast series were performed with a slice thickness of 1.5 mm. The imaging sequences were axial T2-weighted images, diffusion-weighted images, and T1-weighted dynamic contrast-enhancement images. Two independent radiologists evaluated the CEM and MRI images and described the lesions in the contrast-enhanced breast using five features from the Kaiser flowchart:

1. Spiculated/root sign: absent/ present
2. Delayed phase: persistent/ plato/ washout
3. Margins: circumscribed/ irregular

Preprints (www.preprints.org) | NOT PEER-REVIEWED | Posted: 5 May 2023 doi:10.20944/preprints202305.0284.v1

4. Internal enhancement: homogeneous, centrifugal/ inhomogeneous, centripetal
5. Diffuse oedema: absent/ present

The compared CEM and MRI images with histopathologic analysis are shown in Figures 2 and 3. All procedures were performed within 2 weeks of the first suspicious finding on digital mammography, whereas US, CEM and MR were performed 7 days apart. The gold standard was histopathologic analysis. Specimens were obtained by biopsy of the breast lesion with a wide needle under ultrasound guidance. Before the biopsy, subjects were informed about the procedure and possible complications, after which they signed an informed consent. After determining the localization of the lesion by ultrasound and applying local anaesthesia, a biopsy was performed with an automatic gun Biopsy System Hunter 14G, hole length 22 mm (Tsunami Medical, Mirandola, Italy), and the tissue was biopsied until 4 representative samples were obtained. If pathological microcalcifications were found on MG, that had no correlation with US and could not be biopsied under the control of an ultrasound device, VAB was performed. Tissue samples obtained by needle biopsy or VAB were sent for histopathological analysis.

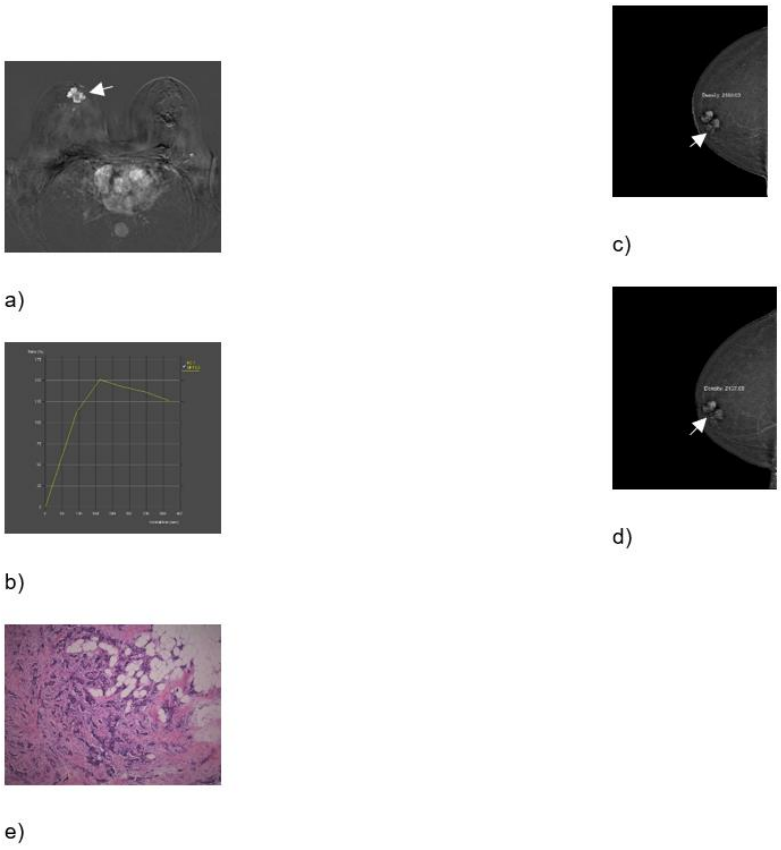

Figure 2. Breast MRI – dynamic contrast-enhanced image: an irregular lesion in the right breast with inhomogeneous, predominantly peripheral enhancement and no oedema (a). Breast MRI – time intensity kinetic curve: this is a type III curve, i.e., washout pattern of the lesion that has a rapid uptake with a reduction in enhancement towards the latter part of the study. It is considered strongly suggestive of malignancy (b). CEM – early recombined CC image of the right breast: an irregular lesion with inhomogeneous, predominantly peripheral enhancement, no oedema, and a mean density value of 2180 (c). CEM – the late recombined image of the right breast: the mean density value of the lesion is 2157, which is a decrease of density of more than 10 units, which indicates washout. It is considered strongly suggestive of malignancy (d). Histopathological analysis - 72-year-old patient underwent a needle biopsy, because the radiologically visualised mass, located in the right breast at the border of the lower quadrants, near the nipple, measuring 3x2.3 cm, radiologically scored as BI-RADS 5. 2 thin cylinders with a total length of 2 cm were obtained by biopsy. Histological analysis

Preprints (www.preprints.org) | NOT PEER-REVIEWED | Posted: 5 May 2023 doi:10.20944/preprints202305.0284.v1

revealed tumour tissue made up of streaks of invasive carcinoma, which was categorized as the 5b category, (HE, ×100) (e).

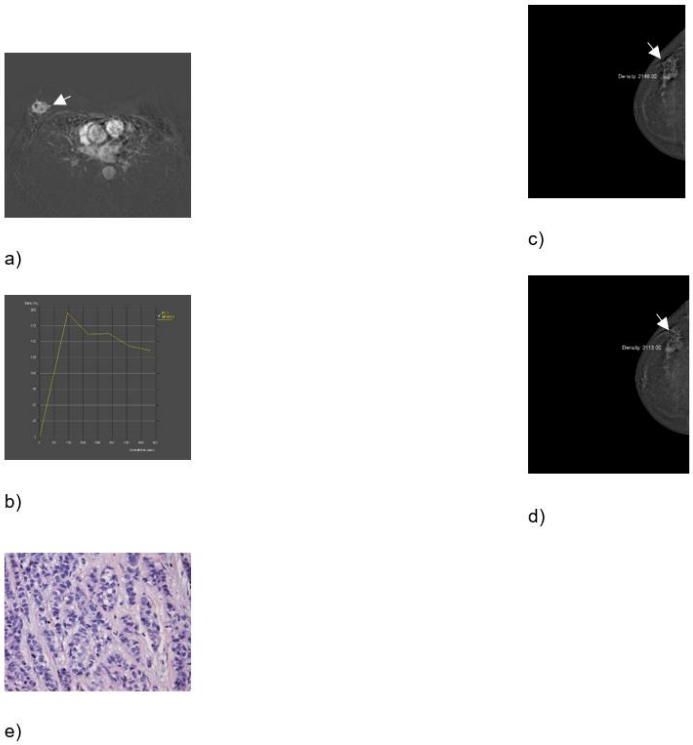

Figure 3. Breast MRI – dynamic contrast-enhanced image: an irregular lesion in the right breast with spiculae, inhomogeneous enhancement, and no oedema (a). Breast MRI – time intensity kinetic curve: this is a type III curve, i.e., washout pattern of the lesion that has a rapid uptake with a reduction in enhancement towards the latter part of the study. It is considered strongly suggestive of malignancy (b). CEM – early recombined CC image of the right breast: an irregular lesion with spiculae, inhomogeneous enhancement, no oedema, and a mean density value of 2148 (c). CEM – late recombined CC image of the right breast: the lesion shows a mean density value of 2113, a decrease of more than 10 units, which indicates washout. It is considered strongly suggestive of malignancy (d). Histopathological analysis - In a 60-year-old patient, a needle biopsy was performed because of a formation, located in the upper lateral quadrant of the right breast, measuring 3.3x1.7 cm, that was radiologically scored as BI-RADS 5. 4 cylinders, with a total length of 6 cm were obtained by biopsy. Histologically invasive breast carcinoma was proven, composed of canaliculi and strings, with solid clusters of atypical epithelial cells, showing moderate cell atypia and a moderate number of mitoses. Such a histological finding was categorized as invasive carcinoma, B5b category of B-diagnostic categories (HE, ×100) (e).

2.4. Clinicopathological data

Patient's clinical data were obtained from electronic medical records: age, sex, 5 CEM/MRI features, microcalcifications on CEM, BI-RADS on MG, type of MG (screening/diagnostic), morphology on MG, type of breast/axilla surgery, the maximum diameter of breast lesion.

Pathologic features included molecular subtypes of breast cancer, the presence of in situ components at diagnosis, and biological features (hormone receptors, proliferation index assessed by Ki67, and HER2 status).

2.5. Statistical analysis

Continuous variables are presented either as mean and standard deviation (SD) for normally distributed data or as median and interquartile range or 95% confidence interval (CI) for data that do

Preprints (www.preprints.org) | NOT PEER-REVIEWED | Posted: 5 May 2023 doi:10.20944/preprints202305.0284.v1

not follow the Gaussian distribution. The normality of distribution was tested using the Shapiro-Wilk test. Categorical variables are presented as counts and percentages. Differences in independent continuous variables between 2 groups were tested for statistical significance with Student's t-test for independent samples or the Mann-Whitney U test, depending on the distribution of the data. Differences between groups on categorical variables were tested for statistical significance using the χ^2test or Fisher's exact test for 2x2 tables. ROC curves were calculated and plotted to evaluate the sensitivity, specificity, positive and negative predictive values, and test accuracy of MRI-derived KS and CEM-derived equivalent. The difference in the n area under ROC curves (ROC-AUC) between diagnostic methods was tested for statistical significance using the DeLong test. The Youden index (*J = sensitivity + specificity - 1*) was used to determine the optimal cut-off values of the KS. However, because of the potentially disastrous consequences of interpreting false-negative findings as true negatives in patients with suspected malignant lesions, only values where 100% true negatives are present are considered clinically acceptable. The sample size was calculated using data from a study by Baltzer et al [14]. The EasyROC v1.3.1. software package was used to calculate the sample size and 47 subjects with confirmed breast cancer and 21 control cases with benign lesions were required to achieve a probability of error of 0.05 and statistical power of 0.8 [15]. The software packages jamovi v2.3.21 and EasyROC v1.3.1. were used for data visualization [16–18]. P values <0.05 were considered statistically significant.

3. Results

This study enrolled 68 subjects who, due to the presence of breast lesions on mammography, underwent US, CEM and MRI in a regional general hospital for 2 years. The mean age was 61.4 ± 11.6 years. There were 47 subjects with biopsy-confirmed malignant lesions and 21 patients with benign lesions. Subjects with breast cancer were older than subjects with benign lesions (64.7 ± 10.8 vs 53.9 ± 9.7 years, P<0.001). In subjects with malignancies, the MRI-derived Kaiser score was 9 (IQR 8-9), its CEM equivalent was 9 (IQR 8-9) and BI-RADS was 5 (IQR 4-5), whereas in subjects with benign lesions, the Kaiser score was 3 (IQR 2-3), it's CEM equivalent was 3 (IQR 1.7-5) and BI-RADS was 3 (IQR 0-4). All scores were significantly higher in subjects with malignancies (P<0.01). ROC-AUC for the MRI-derived Kaiser score was 0.951 and 0.940 for the CEM equivalent. ROC the sensitivity/specificity curves and distribution graphs for CEM-derived Kaiser score are depicted in Figures 4 and 5. As shown in Table 1 and Figure 6, there was no significant difference between ROC-AUC and these two diagnostic methods (P=0.749). The radiological, clinical, and pathohistological characteristics of the malignant lesions are shown in Tables 2 and 3.

Table 1. Properties of receiver operating characteristic curves for MRI KS and its CEM-derived equivalent in discriminating between benign and malignant breast lesions.

	MRI	CEDM
AUC-ROC	0.951	0.940*
Youden cut-off value of Kaiser score	6	6
100% TN Kaiser score	3	3
Sensitivity at Youden cut-off	89.36%	87.23%
Specificity at Youden cut-off	95.24%	95.24%
Accuracy at Youden cut-off	88.2%	86.8%
PPV at Youden cut-off	97.67%	97.62%

Preprints (www.preprints.org) | NOT PEER-REVIEWED | Posted: 5 May 2023 doi:10.20944/preprints202305.0284.v1

NPV at Youden cut-off	80%	76.92%
Specificity at 100% NPV	28.57%	28.57%
PPV at 100% NPV	75.81%	75.81%

* Delong test, P=0.749

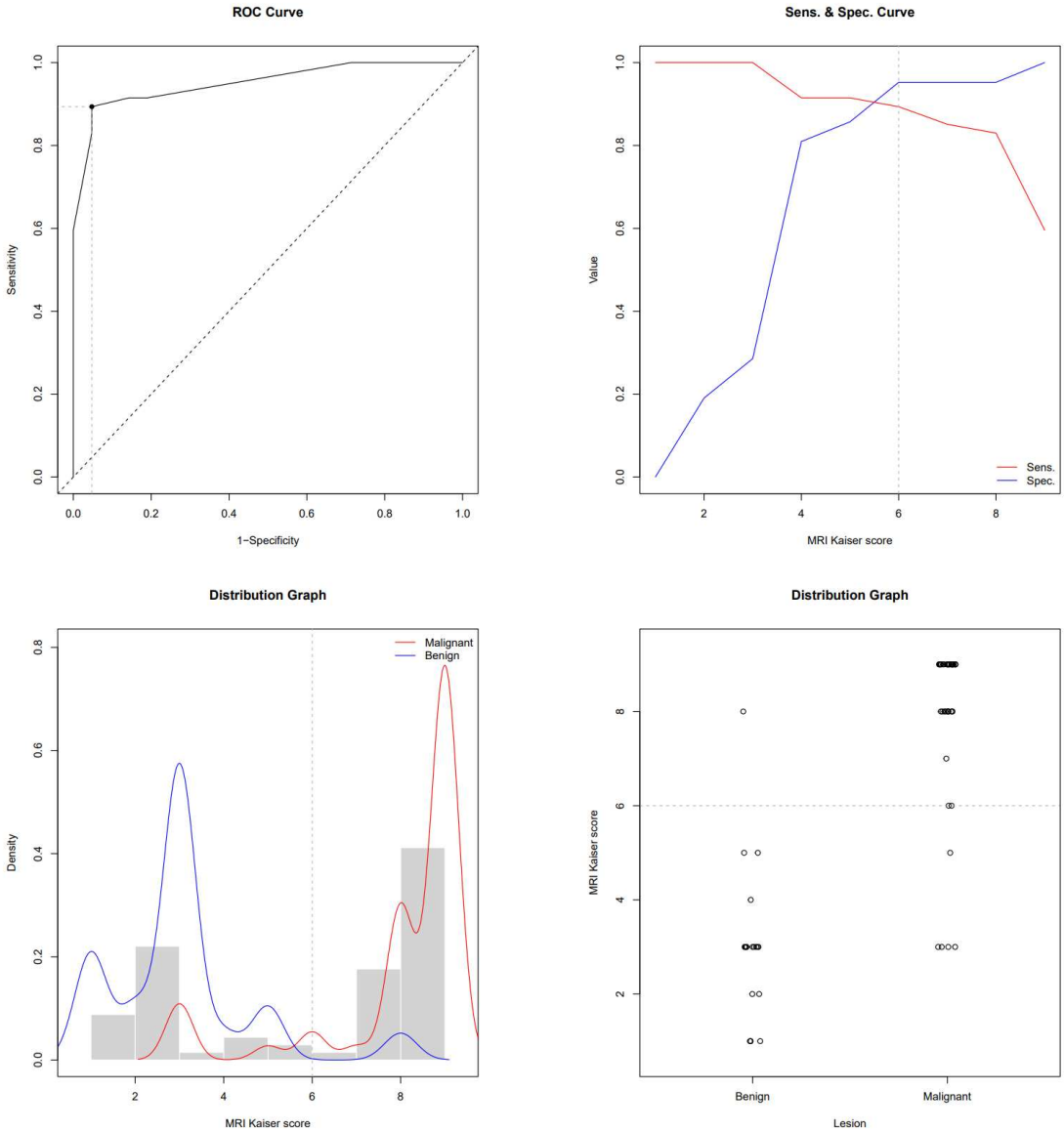

Figure 4. ROC, sensitivity/specificity curves and distribution graphs for MRI Kaiser score, dashed line shows Youden index cut-off (6).

Preprints (www.preprints.org) | NOT PEER-REVIEWED | Posted: 5 May 2023 doi:10.20944/preprints202305.0284.v1

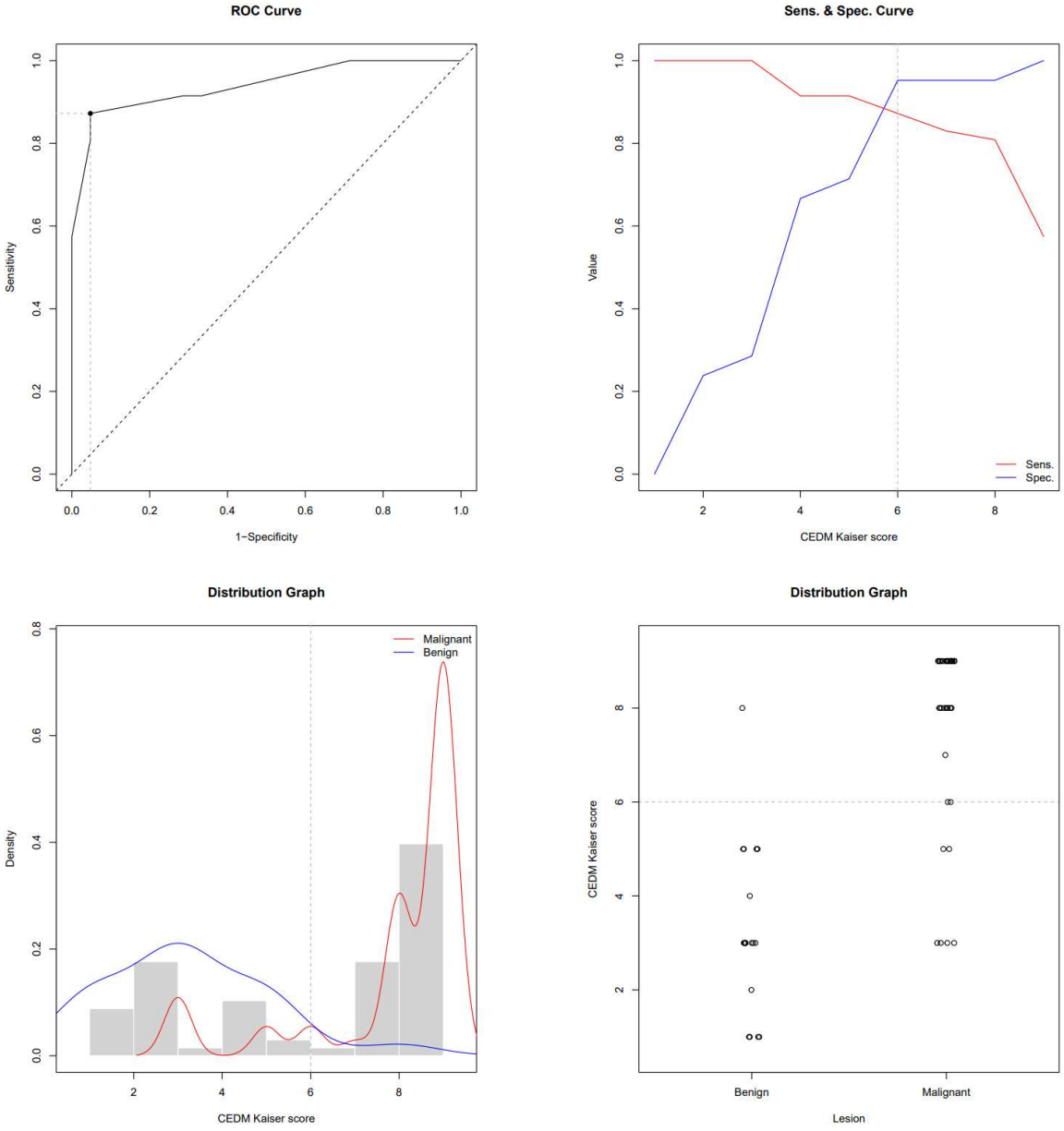

Figure 5. ROC, sensitivity/specificity curves and distribution graphs for CEM-derived Kaiser score, dashed line shows Youden index cut-off (6).

Preprints (www.preprints.org) | NOT PEER-REVIEWED | Posted: 5 May 2023 doi:10.20944/preprints202305.0284.v1

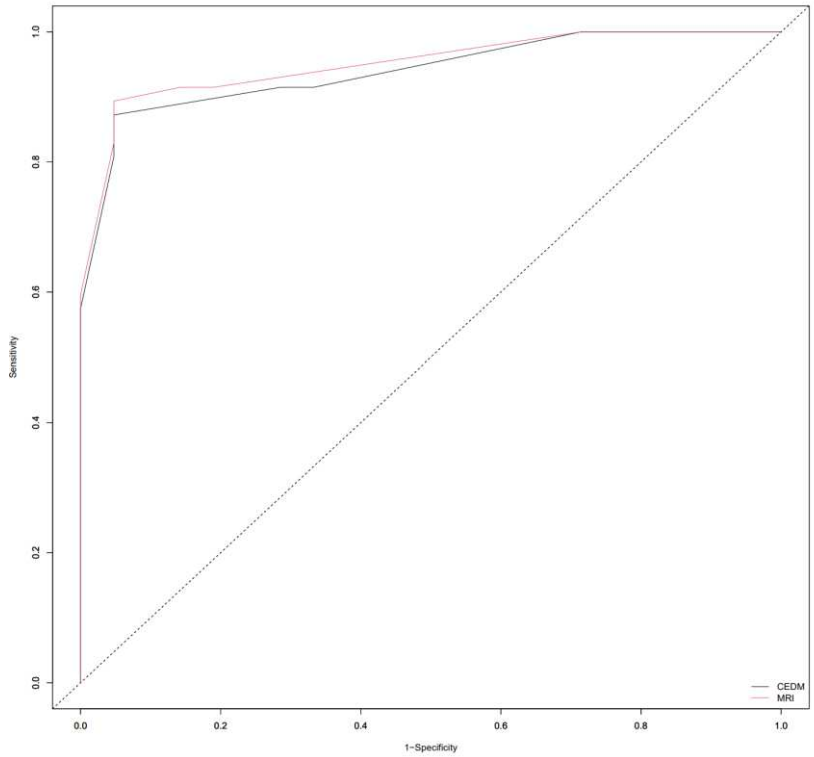

Figure 6. ROC curves depicting differences between ROC-AUC of MRI and CEM-derived Kaiser score.

Table 2. Mammographic, CEM, MRI and clinical characteristics of patients with malignant lesions (N=47).

Mammography BI-RADS	
BI-RADS 3	5 (11%)
BI-RADS 4	12 (26%)
BI-RADS 5	30 (64%)
Type of mammography	
National screening program	13 (28%)
Diagnostic	28 (60%)
MG taken at another institution	6 (13%)
Mammography morphology	
Microcalcifications	3 (6.4%)
Mass	34 (72%)
Mass and microcalcifications	4 (8.5%)
Architectural distortion	2 (4.3%)
Asymmetry (focal asymmetrical density)	4 (8.5%)
Mammography of suspicious axillary lymph nodes	
No	45 (96%)
Yes	2 (4.3%)
CEM microcalcifications	

Preprints (www.preprints.org) | NOT PEER-REVIEWED | Posted: 5 May 2023 doi:10.20944/preprints202305.0284.v1

No	40 (85%)
Yes	7 (15%)
CEM lesion size (mm)	20 (IQR 14, 29)
MRI lesion size (mm)	20 (IQR 14, 28)
Skin Thickening	
No	45 (96%)
Yes	2 (4.3%)
Skin retraction	
No	41 (87%)
Yes	6 (13%)
Reticular subcutaneous tissue	
No	44 (94%)
Yes	3 (6.4%)
Surgical treatment	
SNSM	29 (62%)
RM	12 (26%)
Neoadjuvant therapy + SNSM	3 (6.4%)
Neoadjuvant therapy + RM	3 (6.4%)
Axillary intervention	
None	1 (2.1%)
SLNB	20 (43%)
Dissection	26 (55%)

Table 3. Pathohistological characteristics of patients with malignant lesions (N=47).

PHD	
Invasive lobular Ca + LCIS	7 (15%)
Invasive ductal Ca NST + DCIS	22 (47%)
DCIS	3 (6.4%)
Invasive ductal Ca NST	8 (17%)
Invasive lobular Ca + DCIS	1 (2.1%)
Invasive lobular Ca	3 (6.4%)
Invasive mucinous Ca + DCIS	1 (2.1%)
Invasive mucinous Ca	1 (2.1%)
Invasive tubular Ca	1 (2.1%)
Immunohistochemistry - ER	

 doi:10.20944/preprints202305.0284.v1

No	3 (6%)
Yes	44 (94%)
Immunohistochemistry - PR	
No	5 (11%)
Yes	42 (89%)
Immunohistochemistry - HER2	
No	38 (81%)
Yes	6 (13%)
N/A	3 (6%)
Immunohistochemistry - Ki-67	
Low proliferation (<10%)	12 (25.5%)
Moderate proliferation (10-20%)	12 (25.5%)
High proliferation (>20%)	21 (45%)
N/A	2 (4%)

4. Discussion

Contrast-enhanced mammography is a viable alternative to contrast-enhanced breast MRI [19]. It can serve as an alternative method for patients who are unable to undergo MRI due to contraindication or inaccessibility. Common contraindications to MRI include metal implants, claustrophobia, and weight limitations. Other reasons for incorporating CEM into clinical practice include patient comfort, cost, and accessibility [20].

CEM has comparable performance to breast MRI without the added cost or time of conventional MRI protocols. Therefore, this technique may be useful for indications previously reserved for MRI, such as problem-solving, determining the extent of disease in patients with newly diagnosed cancer, monitoring response to neoadjuvant therapy, evaluating the breast after treatment for residual or recurrent disease, and potentially screening women at intermediate or high risk for breast cancer [20].

This study aimed to evaluate CEM, compare breast lesions on CEM and MRI by 5 characteristics, and develop a flowchart for BI-RADS classification of breast lesions on CEM based on the KS flowchart. KS is an evidence-based decision rule for objectively distinguishing benign from malignant breast lesions. It reflects the increasing likelihood of malignancy and, together with the clinical context, supports individual decision-making [21]. Kang et al. investigated whether KS could improve the diagnostic performance of the BI-RADS system in evaluating breast-enhancing lesions on CEM. They concluded that the use of the KS provided a high diagnostic performance in distinguishing malignant and benign breast lesions on CEM, outperforming BI-RADS and that the use of the KS avoided up to 47.9% of unnecessary biopsies of benign breast lesions [22]. This indicates that a KS-based flowchart for CEM could be a valuable diagnostic tool for breast imaging.

Our study has several limitations. First, it was a prospective study in a single institution. Further prospective studies are needed to investigate the potential of this new CEM flowchart for clinical decision-making. Second, the last criterion in the Kaiser flowchart is “perifocal oedema/diffuse ipsilateral oedema”. The CEM is not capable of representing perifocal edema, so we used only the standard criterion "diffuse ipsilateral breast edema" in the CEM flowchart. Further prospective studies are needed to investigate if this adversely influences the diagnostic performance of the CEM flowchart. Third, we did not investigate the accuracy of special software to measure the dynamics of contrast enhancement in CEM. We used the study by Ainakulova et al. to quantify the enhancement of lesions on CEM: The ROI filter was placed in the most homogeneous area of the lesion on recombinant CEM images acquired after 2 minutes (initial images) and 8 minutes (delayed images).

Based on the difference between the mean value of ROI on the initial and delayed images, three types of lesion enhancement were obtained, which resemble the dynamic curves in breast MRI: 1) persistent enhancement – an increase in the mean value of ROI in the lesion by more than 10 units; 2) plateau enhancement– a change in the mean value of ROI in the lesion by less than 10 units; and 3) washout – a decrease in the mean ROI value in the lesion by more than 10 units [23]. Further prospective studies are needed to investigate whether the ROI enhancement values are concordant with the dynamic curves of breast MRI.

5. Conclusion

There were no significant differences in KS results between CEM and breast MRI. The KS flowchart is applicable in the evaluation of breast lesions on CEM, and a similar flowchart can be created for breast lesions on CEM. The CEM flowchart may facilitate decision-making in daily clinical practice and assist radiologists in standardization, communication and overall clinical performance and patient care.

Funding: This research received no external funding.

Institutional Review Board Statement: The study was conducted according to the guidelines of the Declaration of Helsinki and approved by the Ethics Committee of the Pula General Hospital (Registry Number 2168/01-59-79-19/1-21-8).

Informed Consent Statement: Informed consent was obtained from all subjects involved in the study.

Data Availability Statement: The data presented in this study are available on request from the corresponding author. The data are not publicly available due to ethical reasons.

Conflicts of Interest: The authors declare no conflict of interest.

References

1. Sung H, Ferlay J, Siegel RL, Laversanne M, Soerjomataram I, Jemal A, et al. Global Cancer Statistics 2020: GLOBOCAN Estimates of Incidence and Mortality Worldwide for 36 Cancers in 185 Countries. CA Cancer J Clin. 2021 May;71(3):209–49.
2. Kashyap D, Pal D, Sharma R, Garg VK, Goel N, Koundal D, et al. Global Increase in Breast Cancer Incidence: Risk Factors and Preventive Measures. Biomed Res Int. 2022;2022.
3. Arnold M, Morgan E, Rumgay H, Mafra A, Singh D, Laversanne M, et al. The current and future burden of breast cancer: Global statistics for 2020 and 2040. Breast. 2022 Dec 1;66:15–23.
4. Cardoso F, Kyriakides S, Ohno S, Penault-Llorca F, Poortmans P, Rubio IT, et al. Early breast cancer: ESMO Clinical Practice Guidelines for diagnosis, treatment and follow-up. Annals of Oncology. 2019 Aug 1;30(8):1194–220.
5. Gennari A, André F, Barrios CH, Cortés J, de Azambuja E, DeMichele A, et al. ESMO Clinical Practice Guideline for the diagnosis, staging and treatment of patients with metastatic breast cancer ☆. Annals of Oncology. 2021 Dec 1;32(12):1475–95.
6. Barnard ME, Boeke CE, Tamimi RM. Established breast cancer risk factors and risk of intrinsic tumour subtypes. Vol. 1856, Biochimica et Biophysica Acta - Reviews on Cancer. Elsevier B.V.; 2015. p. 73–85.
7. Phillips J, Fein-Zachary VJ, Slanetz PJ. Pearls and Pitfalls of Contrast-Enhanced Mammography. Journal of Breast Imaging [Internet]. 2019;1(1). [cited 2022 Feb 01]. Available from: https://doi.org/10.1093/jbi/wby013.
8. Nori J, Kaur M. Contrast-enhanced Digital Mammography. Springer International Publishing AG, part of Springer Nature [Internet]. 2018. [cited 2022 Feb 01]. Available from: https://doi.org/10.1007/978-3-319-94553-8.
9. Gelardi F, Ragaini EM, Sollini M, Bernardi D, Chiti A. Contrast-Enhanced Mammography versus Breast Magnetic Resonance Imaging: A Systematic Review and Meta-Analysis. Diagnostics (Basel). 2022 Aug 4;12(8):1890. doi: 10.3390/diagnostics12081890. PMID: 36010240; PMCID: PMC9406751.
10. Kamal, R., Mansour, S., Farouk, A., Hanafy, M., Elhatw, A., Goma, M.M., 2021. Contrast-enhanced mammography in comparison with dynamic contrast-enhanced MRI: which modality is appropriate for whom? Egyptian Journal of Radiology and Nuclear Medicine 52. doi:10.1186/s43055-021-00586-y.
11. Cheung YC, Juan YH, Lin YC et al. Dual-Energy Contrast-Enhanced Spectral Mammography: Enhancement Analysis on BI-RADS 4 Non-Mass Microcalcifications in Screened Women. *PLoS One*. 2016;11(9):e0162740.

12. Contrast-Enhanced Mammography (A supplement to ACR BI-RADS Mammography 2013) [Internet]. [cited 2022 Feb 01]. Available from: https://www.acr.org/.
13. Baltzer, P. A. T., Krug, K. B., & Dietzel, M. (2022). Evidence-Based and Structured Diagnosis in Breasr MRI using the Kaiser Score. RöFo - Fortschritte Auf Dem Gebiet Der Röntgenstrahlen Und Der Bildgebenden Verfahren. https://doi.org/10.1055/a-1829-5985.
14. Baltzer PA, Dietzel M, Burmeister HP, Zoubi R, Gajda M, Camara O, Kaiser WA. Application of MR mammography beyond local staging: is there a potential to accurately assess axillary lymph nodes? evaluation of an extended protocol in an initial prospective study. AJR Am J Roentgenol. 2011 May;196(5):W641-7. doi: 10.2214/AJR.10.4889. PMID: 21512057.
15. easyROC web tool: http://www.biosoft.hacettepe.edu.tr/easyROC/The jamovi project (2022). jamovi. (Version 2.3) [Computer Software]. Retrieved from https://www.jamovi.org.
16. R Core Team (2021). R: A Language and environment for statistical computing. (Version 4.1) [Computer software]. Retrieved from https://cran.r-project.org. (R packages retrieved from MRAN snapshot 2022-01-01).
17. Thiele, C. (2019). cutpoint: Determine and Evaluate Optimal Cutpoints in Binary Classification Tasks. [R package]. Retrieved from https://cran.r-project.org/package=cutpointr.
18. Friesen, L., Kroc, E., Zumbo, B. D. (2019). Psychometrics & Post-Data Analysis: Test ROC. [jamovi module]. Retrieved from https://github.com/lucasjfriesen/jamoviPsychoPDA.
19. Jochelson MS, Lobbes MBI. Contrast-enhanced Mammography: State of the Art. Radiology. 2021 Apr;299(1):36-48. doi: 10.1148/radiol.2021201948. Epub 2021 Mar 2. PMID: 33650905; PMCID: PMC7997616.
20. SoganiJ, Mango VL, Keating D, Sung JS, Jochelson MS. Contrast-enhanced mammography: past, present, and future. Clin Imaging. 2021 Jan;69:269-279. doi 10.1016/j.clinimag.2020.09.003. Epub 2020 Sep 19. PMID: 33032103; PMCID: PMC8494428.
21. Baltzer, P.A.T., Krug, K.B., Dietzel, M., 2022. Evidence-Based and Structured Diagnosis in Breast MRI using the Kaiser Score. RöFo - Fortschritte auf dem Gebiet der Röntgenstrahlen und der bildgebenden Verfahren 194, 1216–1228.. https://doi.org/10.1055/a-1829-5985.
22. Yihe Kang, Zhigang Li, Guang Yang, Jing Xue, Lingling Zhang, Xiaocui Rong, Diagnostic performance of the Kaiser score in the evaluation of breast lesions on contrast-enhanced mammography, European Journal of Radiology, Volume 156, 2022,110524, ISSN 0720-048X, https://doi.org/10.1016/j.ejrad.2022.110524. (https://www.sciencedirect.com/science/article/pii/S0720048X22003746).
23. Ainakulova AS, Zholdybay ZZ, Kaidarova DR, Inozemtceva NI, Gabdullina MO, Zhakenova ZK, Panina AS, Toleshbayev DK, Amankulov JM. Contrast-enhanced spectral mammography without and with a delayed image for diagnosing malignancy among mass lesions in dense breast. Contemp Oncol (Pozn). 2021;25(1):17-22. doi: 10.5114/wo.2021.105030. Epub 2021 Apr 6. PMID: 33911977; PMCID: PMC8063896.